
Citation:

Uslular, G and Ünal, A and Stringer, CD and Nývlt, D and Carrivick, JL and Özsoy, B (2025) Geomorphology of Stansbury Peninsula, Nelson Island, Antarctic Peninsula. *Journal of Maps*, 21 (1). pp. 1-15. ISSN 1744-5647 DOI: <https://doi.org/10.1080/17445647.2025.2532561>

Link to Leeds Beckett Repository record:

<https://eprints.leedsbeckett.ac.uk/id/eprint/12311/>

Document Version:

Article (Published Version)

Creative Commons: Attribution 4.0

© 2025 The Author(s)

The aim of the Leeds Beckett Repository is to provide open access to our research, as required by funder policies and permitted by publishers and copyright law.

The Leeds Beckett repository holds a wide range of publications, each of which has been checked for copyright and the relevant embargo period has been applied by the Research Services team.

We operate on a standard take-down policy. If you are the author or publisher of an output and you would like it removed from the repository, please [contact us](#) and we will investigate on a case-by-case basis.

Each thesis in the repository has been cleared where necessary by the author for third party copyright. If you would like a thesis to be removed from the repository or believe there is an issue with copyright, please contact us on openaccess@leedsbeckett.ac.uk and we will investigate on a case-by-case basis.



Geomorphology of Stansbury Peninsula, Nelson Island, Antarctic Peninsula

Göksu Uslular, Alp Ünal, Christopher D. Stringer, Daniel Nývlt, Jonathan L. Carrivick & Burcu Özsoy

To cite this article: Göksu Uslular, Alp Ünal, Christopher D. Stringer, Daniel Nývlt, Jonathan L. Carrivick & Burcu Özsoy (2025) Geomorphology of Stansbury Peninsula, Nelson Island, Antarctic Peninsula, Journal of Maps, 21:1, 2532561, DOI: [10.1080/17445647.2025.2532561](https://doi.org/10.1080/17445647.2025.2532561)

To link to this article: <https://doi.org/10.1080/17445647.2025.2532561>



© 2025 The Author(s). Published by Informa UK Limited, trading as Taylor & Francis Group on behalf of Journal of Maps



[View supplementary material](#)



Published online: 31 Jul 2025.



[Submit your article to this journal](#)



Article views: 194



[View related articles](#)



[View Crossmark data](#)



RESEARCH ARTICLE



Geomorphology of Stansbury Peninsula, Nelson Island, Antarctic Peninsula

Göksu Uslular ^a, Alp Ünal ^b, Christopher D. Stringer ^{c,f}, Daniel Nývlt ^{d,e}, Jonathan L. Carrivick ^f and Burcu Özsoy ^{a,g}

^aPolar Research Institute, TÜBİTAK Marmara Research Center, Kocaeli, Türkiye; ^bDepartment of Geological Engineering, Faculty of Mines, İstanbul Technical University, İstanbul, Türkiye; ^cSchool of the Built Environment, Engineering and Computing, Leeds Beckett University, Leeds, UK; ^dPolar-Geo-Lab, Department of Geography, Faculty of Science, Masaryk University, Brno, Czechia; ^eCzech Geological Survey, Brno Branch, Brno, Czechia; ^fSchool of Geography and water@leeds, University of Leeds, Leeds, UK; ^gDepartment of Maritime Transportation and Management Engineering, Faculty of Maritime, İstanbul Technical University, İstanbul, Türkiye

ABSTRACT

The proglacial landscapes of Antarctica offer critical insights into past and ongoing deglaciation processes and the impacts of climate change. This study presents the first geomorphological map of the proglacial part of Stansbury Peninsula (Rip Point) and Cariz Cabo Cape in the northern part of Nelson Island. We identify and characterise a variety of glacial, proglacial, paraglacial, and periglacial landforms using high-resolution drone imagery, fieldwork, and geological data. The defined landforms presented reflect a complex interplay of erosional and depositional processes shaped by multiple glacial advance-retreat cycles since the Last Glacial Maximum, with evidence for significant glacial activity during the Holocene. The presence of hyaloclastite and crystalline erratic boulders further contributes to the reconstruction of glacial dynamics in the region. Our findings provide a crucial dataset and baseline for studies on future Antarctic deglaciation, periglacial processes, and the expansion of proglacial landscapes driven by ongoing climate change.

ARTICLE HISTORY

Received 27 May 2025
Revised 1 July 2025
Accepted 4 July 2025

KEYWORDS

Geomorphological mapping; deglaciation; periglacial landforms; South Shetland Islands; Antarctic Peninsula

1. Introduction


Proglacial landscapes comprise just 0.18% of the total Antarctic continent (Burton-Johnson et al., 2016), but contain distinct landform products of deglaciation and therefore important evidence of climate change. Deglaciation has been ongoing since the Last Glacial Maximum (LGM) with different cyclic episodes across western Antarctica (Cofaigh et al., 2014; Heroy & Anderson, 2007; Nývlt et al., 2020). This deglaciation, combined with rising temperatures (Vaughan et al., 2003), is producing biological diversity and ecosystem development (e.g. Convey, 2010; Roland et al., 2024; Stringer et al., 2025). Similarly, geomorphological and geological mapping of proglacial landscapes and monitoring of their temporal and spatial changes are very important for understanding the dynamics of the cryosphere and the consequences of global climate change (Chandler et al., 2018; Jennings et al., 2021; Oliva et al., 2019; Oliva & Ruiz-Fernández, 2017; Yıldırım, 2020).

Proglacial regions are critical to advancing our understanding of climate-driven landscape changes in Antarctica (e.g. Carrivick & Tweed, 2013; Heckmann et al., 2016; Kavan et al., 2023; Stringer et al., 2025; Zimmer et al., 2022). Because of their highly dynamic

characteristics shaped by glacial melt, sediment transport and permafrost thaw, they act as key zones of sediment and solute release (Carrivick & Tweed, 2021; Kavan et al., 2017; Stringer et al., 2024), with significant implications for terrestrial, fluvial and marine ecosystems (Orwin & Smart, 2004). Producing robust, site-specific landform and land cover maps is therefore essential for monitoring landscape evolution and anticipating ecological shifts under ongoing climate change (Carrivick et al., 2018; Corte et al., 2024).

The South Shetland Islands (SSI), located in the northwestern part of the Antarctic Peninsula Region (APR), encompass several significant proglacial landscapes. Most of these landscapes observed along the margins of the SSI have developed during the early-mid Holocene (9-6 ka; Heredia Barión et al., 2023; Oliva et al., 2019, 2023), corresponding to the Holocene Thermal Maximum (Renssen et al., 2012). Recent studies on the geomorphological mapping of the larger areas in the SSI (e.g. Fildes Peninsula, Barton Peninsula) have documented extensive periglacial landforms, many of which show signs of recent degradation (López-Martínez et al., 2012). However, smaller and less-studied proglacial landscapes in the SSI and APR, which are key components in understanding the impacts of both past and ongoing environmental

CONTACT Göksu Uslular  goksu.uslular@tubitak.gov.tr

 Supplemental map for this article is available online at <https://doi.org/10.1080/17445647.2025.2532561>.

© 2025 The Author(s). Published by Informa UK Limited, trading as Taylor & Francis Group on behalf of Journal of Maps

This is an Open Access article distributed under the terms of the Creative Commons Attribution License (<http://creativecommons.org/licenses/by/4.0/>), which permits unrestricted use, distribution, and reproduction in any medium, provided the original work is properly cited. The terms on which this article has been published allow the posting of the Accepted Manuscript in a repository by the author(s) or with their consent.

changes, remain poorly understood, particularly with respect to the spatial distribution and characteristics of their landforms.

In this study, we present the first detailed geomorphological map of Stansbury Peninsula (Rip Point), situated in the northern part of Nelson Island (northern SSI), a region where geological and geomorphological characteristics remain poorly understood (Bastías et al., 2023; Gao et al., 2018; Li et al., 1996; Meier et al., 2023; Xiangshen & Xiaohan, 1990). Using high-resolution, drone-based models and field observations, supported by a new virtual tour of the site, we comprehensively map both geological and geomorphological features, revealing new insights into the effects of deglaciation on landform evolution in Stansbury Peninsula. The resulting map and related geomorphological descriptions will contribute to our understanding of the spatial dynamics of deglaciation processes in the northern SSI and, more importantly, serve as a foundation for future research in Antarctic proglacial regions.

2. Study area

Nelson Island is located at the middle of the SSI, northwestern tip of the AP (Figure 1A and B) and is

separated from King George Island by the narrow Fildes Strait (~500 m wide; Figure 1C). The island, with a total area of 165 km², is predominantly covered by the Nelson Ice Dome that occupies approximately 95% of the island (Jiawen et al., 1995; Xiaodong et al., 2004) (Figure 1C). There are three major proglacial landscapes along the northern, western, and eastern coasts: Rip Point (also known as Stansbury Peninsula; ~3 km²) and Cariz Cabo Cape (0.5 km²), Harmony Point (4.5 km²), and Duthoit Point (2.5 km²), respectively (Figure 1C). Harmony Point is classified as an Antarctic Specially Protected Area (ASP 133) and is the most studied region in terms of geology and biology (e.g. da Rosa et al., 2022; Oosthuizen et al., 2020; Rodrigues et al., 2019).

Nelson Island experiences a polar maritime climate, but direct meteorological data were not available until 2021, when an automated weather station was installed close to CZ*ECO-Nelson camp of the Czech Republic (Figure 1C). The meteorological data collected by the Czech Antarctic Research Programme for 2022–2023 (calendar year) (Neznajová, 2024) recorded that the daily mean temperatures range between −14°C and +8°C, and the mean annual air temperature was −1.2°C. The minimum and maximum

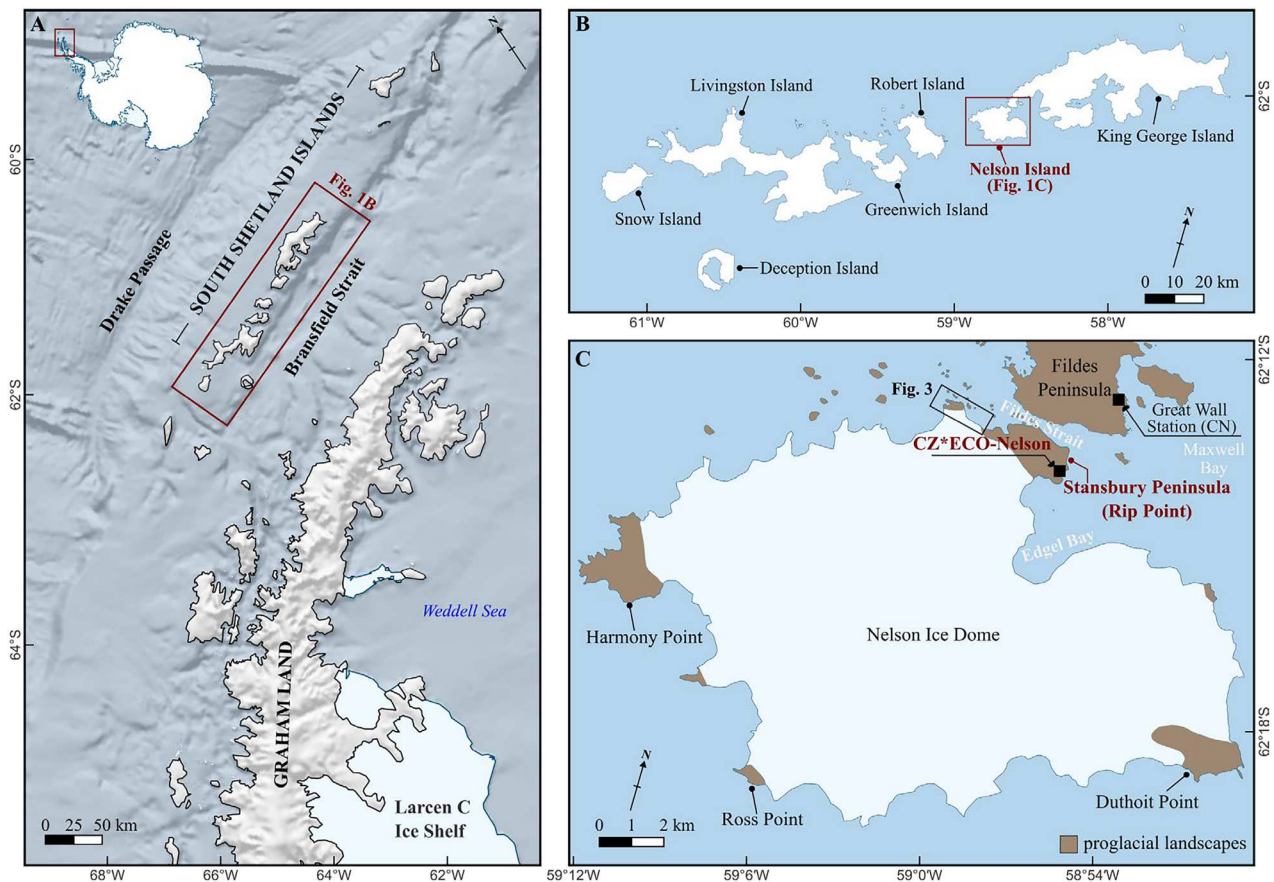


Figure 1. Maps depicting (A) the central and northern sectors of the Antarctic Peninsula, western Antarctica; (B) the South Shetland Islands; and (C) Nelson Island, highlighting the study area at Stansbury Peninsula along with other proglacial landscapes and the surrounding ice dome. Digital elevation models (ETOPO1; Amante & Eakins, 2009), geographic boundaries, proglacial landscape and location names are from the Quantarctica database (Matsuoka et al., 2021) and the SCAR Composite Gazetteer of Antarctica (SCAR, 2014), respectively.

temperatures measured were -15.3°C and 8.7°C , respectively. Typically, daily mean temperatures are approximately zero (-2 – 2°C recorded in 61% of days). These data show a low temperature variability compared to other parts of Antarctica. Local climate is also characterised by high relative humidity, which oscillated mostly between 90 and 100%, with the average of 93.5% and the lowest measured relative humidity of 53.5%. A relative humidity of 100% was recorded on $\sim 65\%$ of days.

The glacial history and geomorphological characteristics of Nelson Island remain poorly documented. Available data for the ice dome indicate that it is relatively thin (~ 120 m thick in 1989) and is sustained by high levels of precipitation driven by mild atmospheric temperatures and the influence of proximal marine air masses (Jiawen et al., 1995). The Island exhibits glaciological and geomorphological features analogous to those observed on the Fildes and Barton Peninsulas, in the south of King George Island (Figure 1B–C). The deglaciation of these areas, where the periglacial landforms are dominant (López-Martínez et al., 2012), initiated around 9–6 ka (Heredia Barión et al., 2023; Oliva et al., 2019, 2023).

The main lithology on Stansbury Peninsula (Nelson Island) displays similarities with the Fildes Peninsula Group (Bastías et al., 2023; Gao et al., 2018; Li et al., 1996; Xiangshen & Xiaohan, 1990). Following the geological map of Li et al. (1996), recent studies correspond the outcrops in the region to the Fossil Hill (middle Eocene; Mansilla et al., 2014) and Jasper Hill (early Eocene; Gao et al., 2018) Formations, consisting of volcanic breccia, tuff and volcanoclastic deposits and mafic lavas and breccias, respectively (Bastías et al., 2023; Gao et al., 2018). In addition, sub-volcanic bodies are observed in several parts of the region.

3. Materials and methods

The geomorphological map of the study area was developed using high-resolution (~ 3 cm/px) orthomosaic and Digital Elevation Model (DEM), complemented by a February 2006 Google Earth image and fieldwork conducted in February 2023, a period when snow and ice coverage are at their annual minimum. Airborne surveys were conducted using DJI Mavic 3 Pro and DJI Phantom 4 Multispectral drones. The structure from Motion-Multi View Stereo (SfM-MVS; Bemis et al., 2014; Carrivick et al., 2013; Carrivick et al., 2016; Smith et al., 2016) techniques were employed for processing drone images, resulting in high-resolution 3D terrain models. Ground control points (GCPs) were established using Real-Time Kinematic (RTK) differential Global Positioning System (dGPS) positioning integrated within the drone, supplemented by ground-surveyed georeferenced points

comprising A0-sized cardboard plates. To extend spatial resolution and enhance the 3D analysis, we incorporated the 4 m-resolution Reference Elevation Model of Antarctica (REMA; Howat et al., 2019). Several vector layers from the Quantarctica database (Matsuoka et al., 2021) were used as basemap features, while geographic names were primarily obtained from the SCAR Composite Gazetteer of Antarctica (SCAR, 2014).

Our approaches to mapping glacial landforms in the study area are outlined in Chandler et al. (2018). Coordinates of distinct geomorphological features, recorded during fieldwork by handheld GPS devices or mobile phone applications, were used to identify these features on drone-derived orthomosaics and DEMs. Additionally, a georeferenced 360° image dataset presented as a virtual tour (Supplemental Materials) provided further contextual information. Terrain analyses were performed using the drone-based DEM, generating hillshade, slope and curvature maps. These analyses facilitated the identification and mapping of geomorphological features, following approaches similar to those described in the literature (e.g. Ely et al., 2017; Smith et al., 2016; Smith & Clark, 2005). For instance, slope values $> 15^{\circ}$ were used as preliminary indicators of moraine ridges, while low-slope, high-concavity areas suggested the presence of braidplains. Mapped features manually digitalised at a scale of 1:500–1:1000 using QGIS (Quantum Geographic Information System) were also compared with those mapped in nearby areas (e.g. Dąbski et al., 2017; Francelino et al., 2011; López-Martínez et al., 2016; Oliva et al., 2019) and across the Antarctic Peninsula (Jennings et al., 2021; Yıldırım, 2020) to ensure their robustness. Further adjustments were made based on visual confirmation in orthomosaics and field observation.

Glacial landforms within the study area were classified into three main categories: proglacial, paraglacial and periglacial (Ballantyne, 2002; Slaymaker, 2009, 2011). Other landforms, affected by structural and geological processes, were also identified, many of which have been significantly shaped by past glacial activity. The criteria used to distinguish and define these landforms are summarised in the Supplementary Table, with further details provided in the following sections.

4. Results

Here, we provide the first detailed geomorphological map of Stansbury Peninsula and Cariz Cabo Cave, including features of various glacial landforms (Main Map, Figures 2 and 3). In the following sections, we briefly describe each mapped component, including structural, glacial, proglacial, paraglacial and periglacial landforms and deposits.

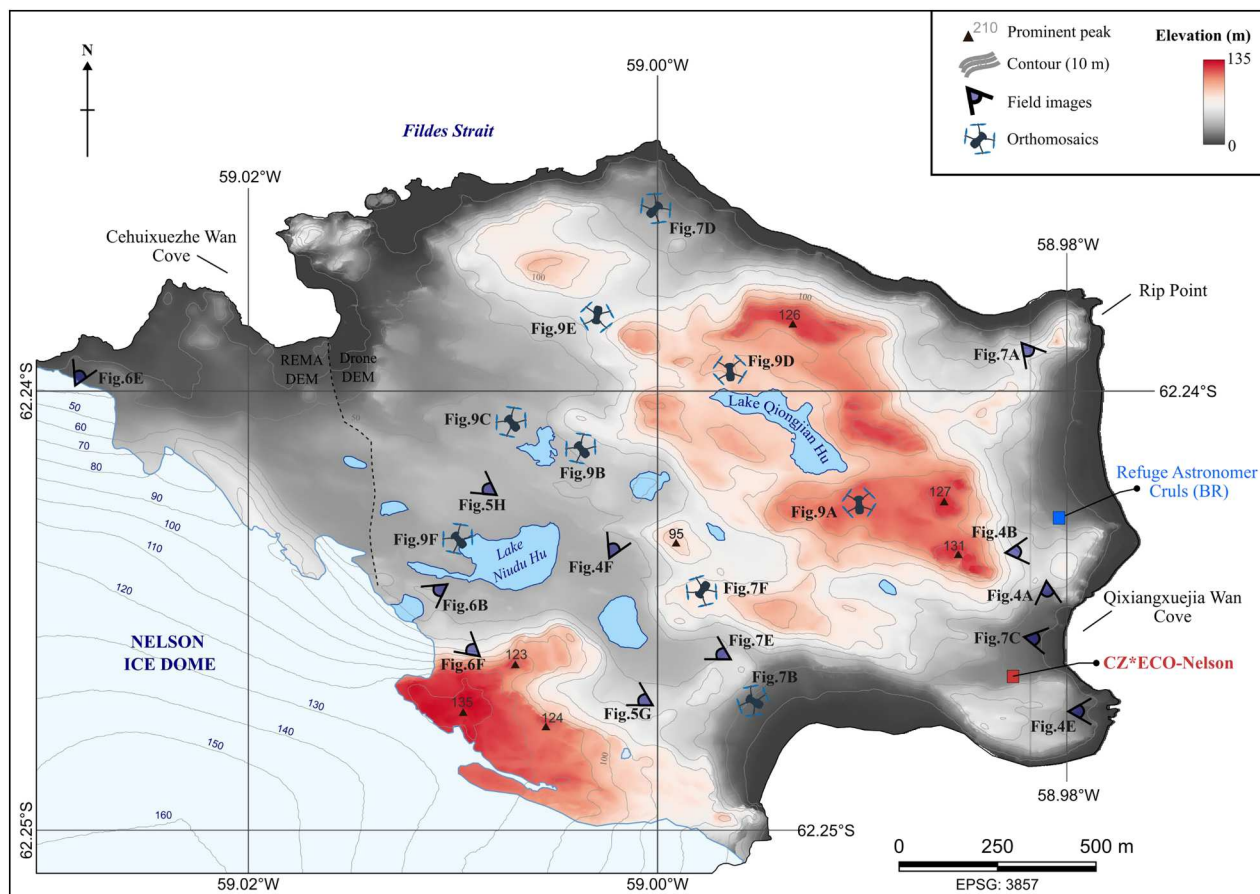


Figure 2. Digital elevation models of Stansbury Peninsula highlight the elevated mesas/platforms in the eastern and southern sectors. The locations of field images and orthomosaics displayed in the following figures are shown by different symbols. The dashed line represents the boundary between REMA (4 m-resolution; Howat et al., 2019) and drone-based (~3 cm/px) DEMs. See the Main Map for the details of geomorphological features.

4.1. Geological features with geomorphological expressions

4.1.1. Volcanic landforms and surface processes

Mesa-like platforms are the dominant elevated landforms, with the upper platforms (80–135 m) primarily occupying the northern, southern, and eastern sectors of Stansbury Peninsula, and the lower platforms (40–70 m) located in the western sector (Main Map and Figures 2 and 4A). Rock cliffs, which are particularly eroded, are mainly exposed along the coastal areas (Main Map and Figures 2 and 4B). Sill-like intrusions are visible in some of the rock cliffs, which are interpreted as volcanic plugs (Figure 4B). The extensive erosional processes, together with freeze–thaw weathering, especially near the coast of Cariz Cabo Cape result in the formation of volcanic stacks (Figure 4C and D). In addition, the sub-volcanic dykes and columnar jointing lava flows are common especially in the lower platform areas (Figure 4E and F).

4.1.2. Lithological and structural characteristics

The dominant volcanic rock landform types on Stansbury Peninsula are basaltic and basaltic-andesitic lava flows, particularly concentrated in the southern and

southeastern parts. These lava flows exhibit prominent columnar jointing, with columns dipping at 10–15° and displaying linear, uniform geometries that differ from typical radial formations (Figure 4F). In the central-eastern sectors, dark grey to black porphyritic lavas containing plagioclase phenocrysts are widespread. These commonly exhibit vesicular and amygdaloidal textures and may correlate with the early Eocene Jasper Hill Formation (Gao et al., 2018), constituting a significant portion of erosional sedimentary surfaces in Stansbury Peninsula.

Volcanic breccias, particularly abundant in the northeastern and southeastern parts of the Stansbury Peninsula, consist of red-brown, sub-angular to sub-rounded basaltic lava fragments and blocks, up to 1.5 m in size. These breccias often overlie agglomerate deposits, including sub-rounded volcanic clasts. Pyroclastic and volcanoclastic deposits in the region are represented by tuffs and rarely interbedded shales. These deposits are mostly exposed in the central and northwestern parts of Stansbury Peninsula and potentially correspond to the Fossil Hill Formation (middle Eocene; Mansilla et al., 2014).

Intrusive bodies are also common throughout the study area and include small stocks, plug-like

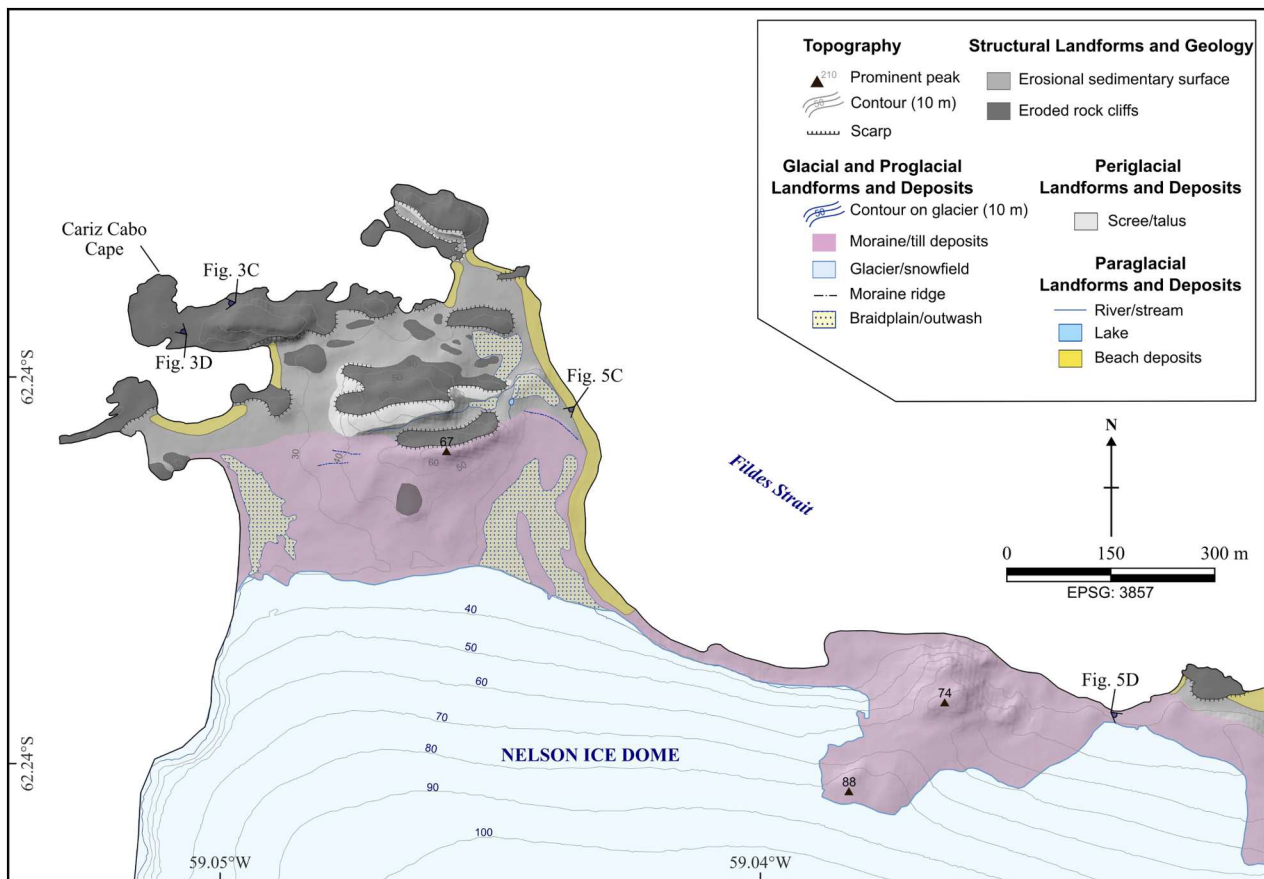


Figure 3. Geomorphological map of the Cariz Cabo Cape, consisting predominantly of rock cliffs, where penguin colonies exist. Hillshade used in the background was derived from the REMA DEM (4 m-resolution; [Howat et al., 2019](#))

intrusions, and NW-SE trending mafic dykes ([Figures 3 and 4B and E](#)). The plug-like intrusions, found at the eastern and western edges of the peninsula, are mafic in composition and display porphyritic texture. Some of these intrusions appear to have acted as feeder conduits, as they show interfingering with overlying lava sequences. Two gabbroic stocks observed in the region are crosscut by the volcanic breccias, suggesting a complex contact relationship.

Linear mafic dykes with a NW-SE strike are particularly abundant, cutting through all main lithological units. Some of the best-preserved dykes, found about 500 m south of the CZ*ECO-Nelson (CZE) base, exhibit well-developed chilled margins and range up to 1 metre in thickness ([Figure 4E](#)).

4.2. Geomorphological features

4.2.1. Glacial landforms and deposits

Melt ponds and crevasses are the main features observed on the surface of Nelson Ice Dome ([Figure 5A-C](#)). Melt ponds are shallow water bodies from surface melting and ponding in depressions on glaciers, while some include dark-coloured sediments interpreted as cryoconites ([Figure 5B and C](#)). Crevasses are deep linear cracks, indicating active ice movement and internal stress within the glacier. The terminus face is a steep ice cliff, ~5 m high, and the presence

of icebergs at calving front indicates that the glacier is dynamically active ([Figure 5A](#)).

In addition to moraine/till deposits mostly observed along the calving front of the Nelson Ice Dome ([Figure 5](#)), steep hillslopes composed of unsorted supraglacial debris are also present. These moraines, which are accumulations of glacially transported debris, are characterised by large blocks embedded within a finer-grained matrix ([Figure 5D](#)). These blocks are mostly volcanic in origin but also include different lithologies. Such deposits are best observed in the southern part of the Cariz Cabo Cape ([Figure 5D](#)).

Erratic blocks of diverse lithologies and sizes are scattered throughout the region, particularly along the coast and within Stansbury Peninsula. These are generally large boulders transported by glacial ice and deposited far from their bedrock source, offering further insights into former ice flow paths. On the eastern coast, granite boulders and volcanic bombs are evident, while green-coloured crystalline boulders and glassy hyaloclastite boulders dominate the erratics within the inner parts of Stansbury Peninsula ([Figure 5E and F](#)).

Another common feature in the Stansbury Peninsula is polished, jointed, and striated bedrock surfaces, shaped by glacial abrasion ([Figure 5G and H](#)). These glacially abraded surfaces exhibit linear grooves and polish that indicate former ice movement directions. They are often associated with intense physical weathering caused

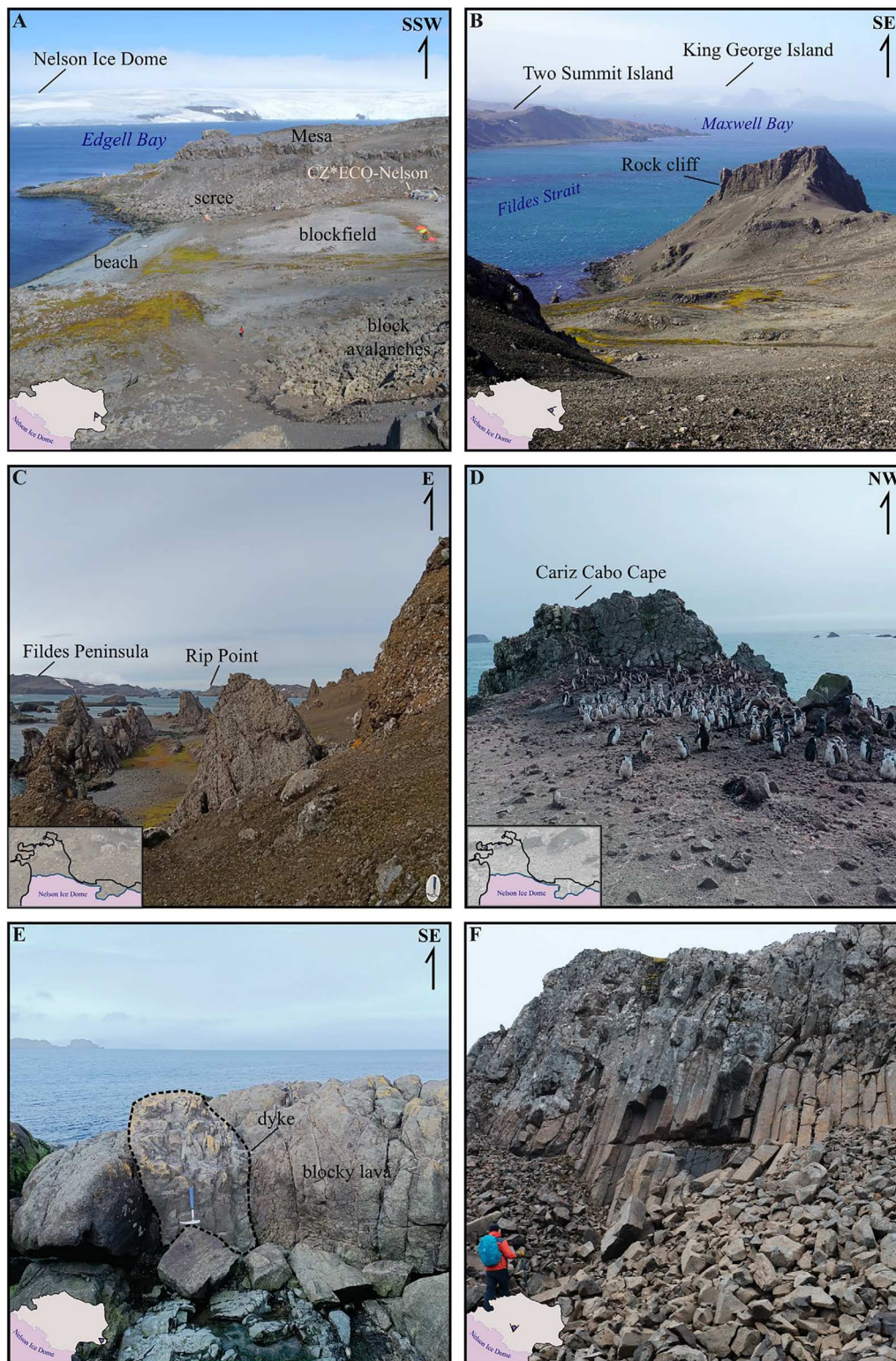


Figure 4. General view of the geological landforms and deposits. **A.** View from SSE showing the geomorphological characteristics with mesa-like platforms, blockfields, scree slopes, and block avalanches. **B.** Coastal rock cliff near Fildes Strait with steeply exposed lava flows and a sill-like volcanic plug. **C-D.** Volcanic stacks at Cariz Cabo Cape, interpreted as remnants of volcanic rock outcrops. **E.** Sub-volcanic dyke intrudes into the blocky lava flow. **F.** Columnar-jointed lava flows in the lower platform, with scree accumulation at the base, potentially due to freeze-thaw weathering and gravitational mass wasting.

by freeze-thaw processes, leading to the development of discontinuous ridgelines (Figure 5I).

4.2.2. Proglacial landforms and deposits

Proglacial landforms and deposits in the study area are predominantly outwash plains and braidplains, with

few kames and kettle ponds (Figure 6). The outwash plains are broad, gently sloping surfaces formed by meltwater streams that deposited sorted sands and gravels beyond the glacier margin. These are commonly associated with braidplains, which are the networks of intertwining meltwater channels that redistribute

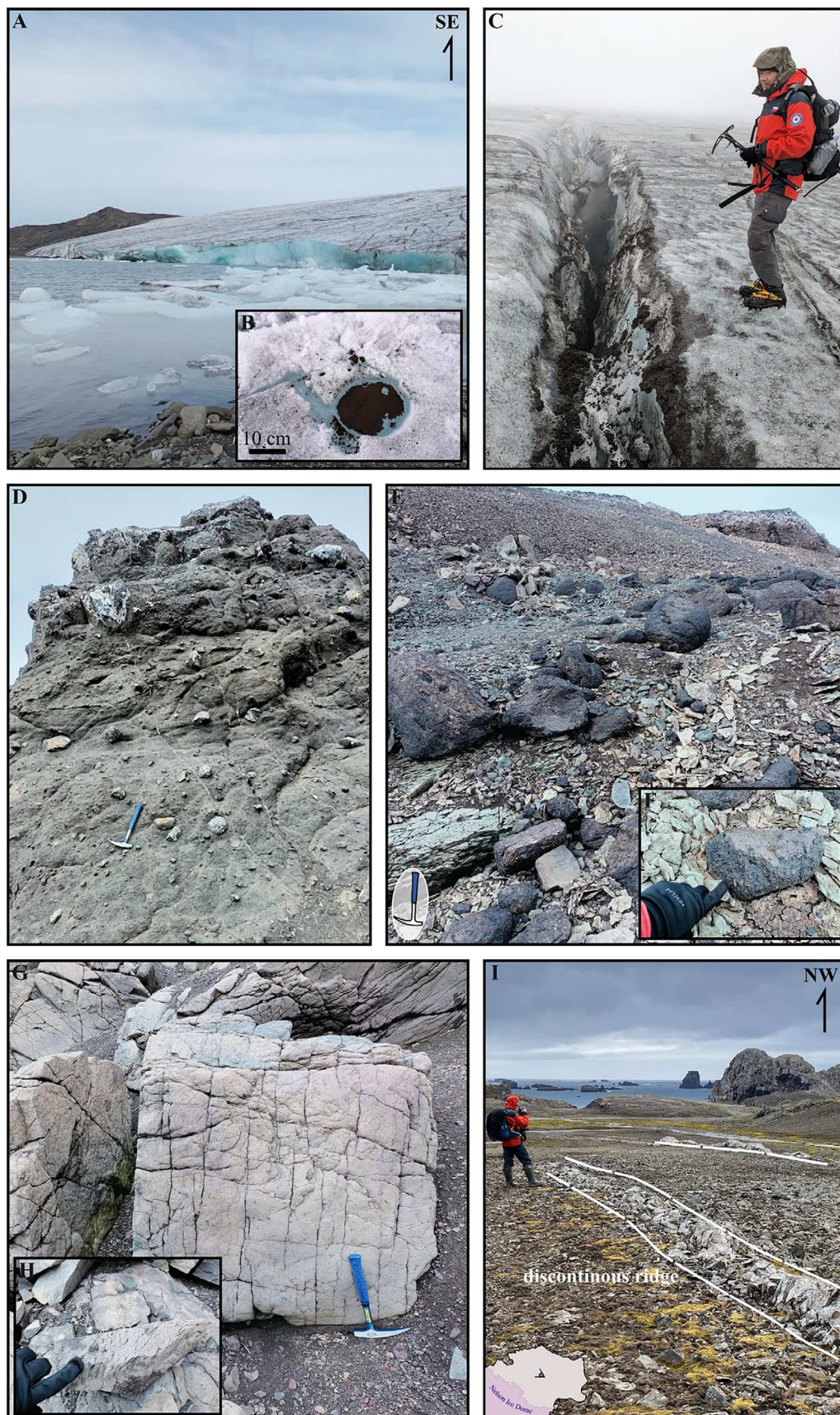


Figure 5. The common glacial landforms in the study area illustrate various aspects of past and recent glacial dynamics. **A.** Calving front of a glacier, with floating ice chunks visible over the sea, indicating active deglaciation. **B.** A melting pond observed on the glacier surface, including supraglacial debris (or cryoconite). **C.** Crevasses filled mostly by supraglacial debris. **D.** Till deposits consist of poorly sorted sediments and erratic blocks with varying origins. **E.** Blockfield within the Stansbury Peninsula comprises hyaloclastite and green-coloured crystalline boulders. **F.** The close-up view of a hyaloclastite boulder displaying a glassy texture. **G.** Glacial striations on a rock body, evidence of abrasion caused by the glacial retreat. The geological hammer is a scale (40.7 cm). **H.** Close-up view of striations on rocks. **I.** Eroded moraine ridges observed in NW parts of the Stansbury Peninsula.

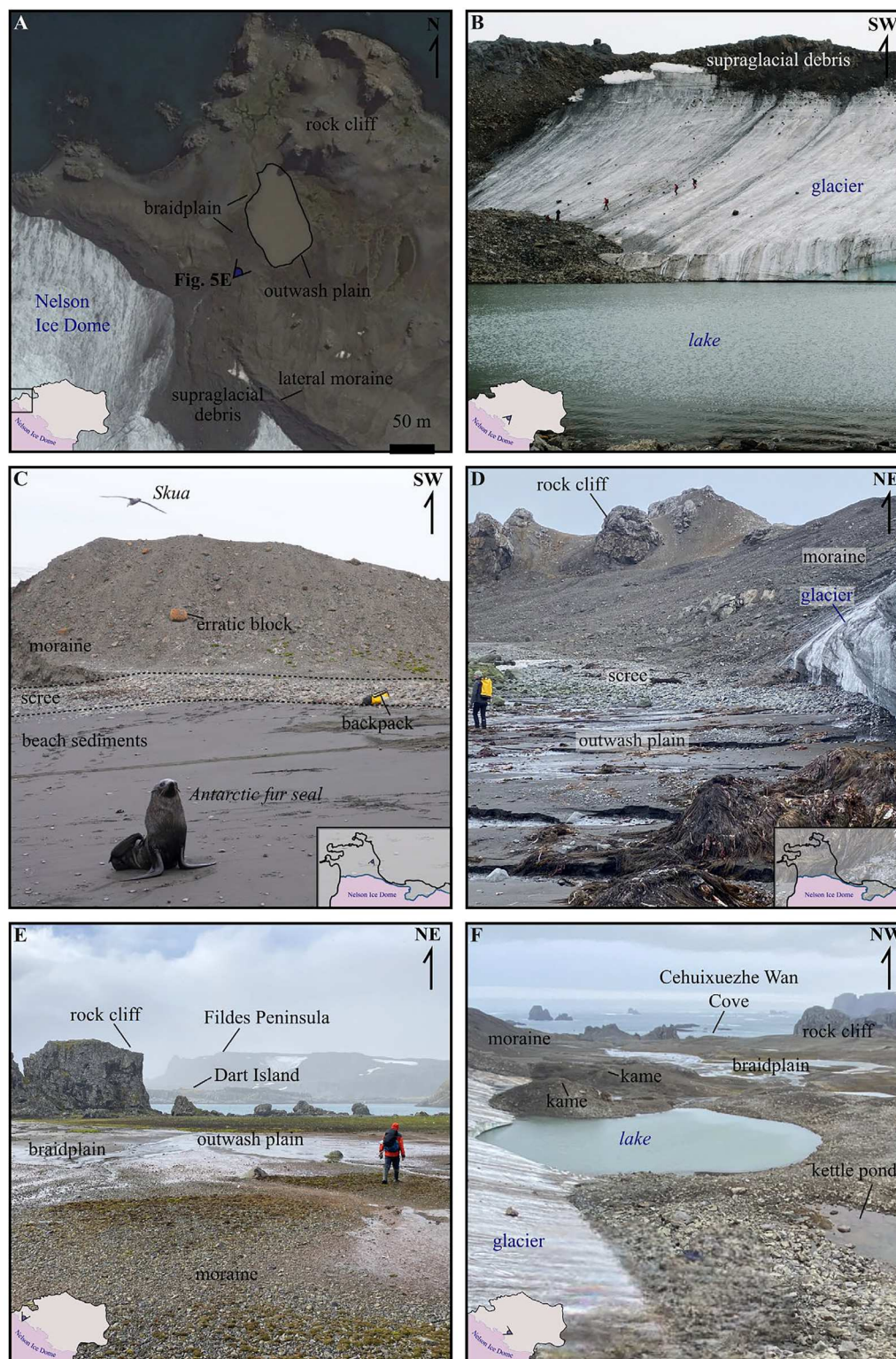


Figure 6. Key proglacial landforms and deposits in the study area. **A.** Google Earth view of the northern parts of the Stansbury Peninsula, showing eroded rock cliffs, braidplain, and outwash plain, along with till deposits and a lateral moraine. **B.** The steep-sloped supraglacial debris over the glacial terminus. **C.** Poorly sorted proglacial till deposits from the Cariz Cabo Cape include erratic blocks, with beach sediments and talus slopes in the foreground, where an Antarctic fur seal is present. **D.** Proglacial moraine deposits at the base of a rock cliff, with debris flows feeding into the outwash plain, adjacent to the calving front of Nelson Ice Dome. **E.** North-eastward view of the area in A, with Fildes Peninsula and Dart Island in the background. **F.** North-westward view of Cehuixuezhe Wan Cove, displaying proglacial features such as kames and kettle ponds, with rock cliffs and paraglacial landforms in the background.

glacial debris across the proglacial zone. Moraines, which are ridges of glacial debris deposited at or near the glacier margin, are predominantly distributed along the proglacial environment of the Nelson Ice Dome, particularly along the western and southern

margins of the Stansbury Peninsula and Cariz Cabo Cape, respectively (Main Map, Figures 3 and 6A-C). Moraines at steep slopes with lateral ridges (i.e. recessional moraines) on the peninsula tend to be ice-cored and likely represent more recent glacial activity

(Figure 6B), whereas those at lower slopes with well-defined ridgelines (i.e. push moraines), especially prominent at Cariz Cabo Cape, may indicate older glacial episodes (Figure 6C). Meltwater and debris derived from the glacier and adjacent moraines are transported into the outwash plains via braided river systems, obviously evident along the coastline and within the Cariz Cabo Cape (Figure 6D and E). Near the glacier terminus on the peninsula, the presence of kames and kettle ponds further reflects a complex post-glacial

depositional environment (Figure 6F). Kames are mounds or hummocks of sand and gravel deposited by meltwater, while kettle ponds form when blocks of ice become buried by outwash sediment and later melt.

4.2.3. Paraglacial landforms and deposits

The raised beaches, marine terraces, scree/talus slopes, drift-mantled slopes, and block avalanches are the most common paraglacial landforms and deposits (Ballantyne, 2002) observed in the study area (Figure 7).

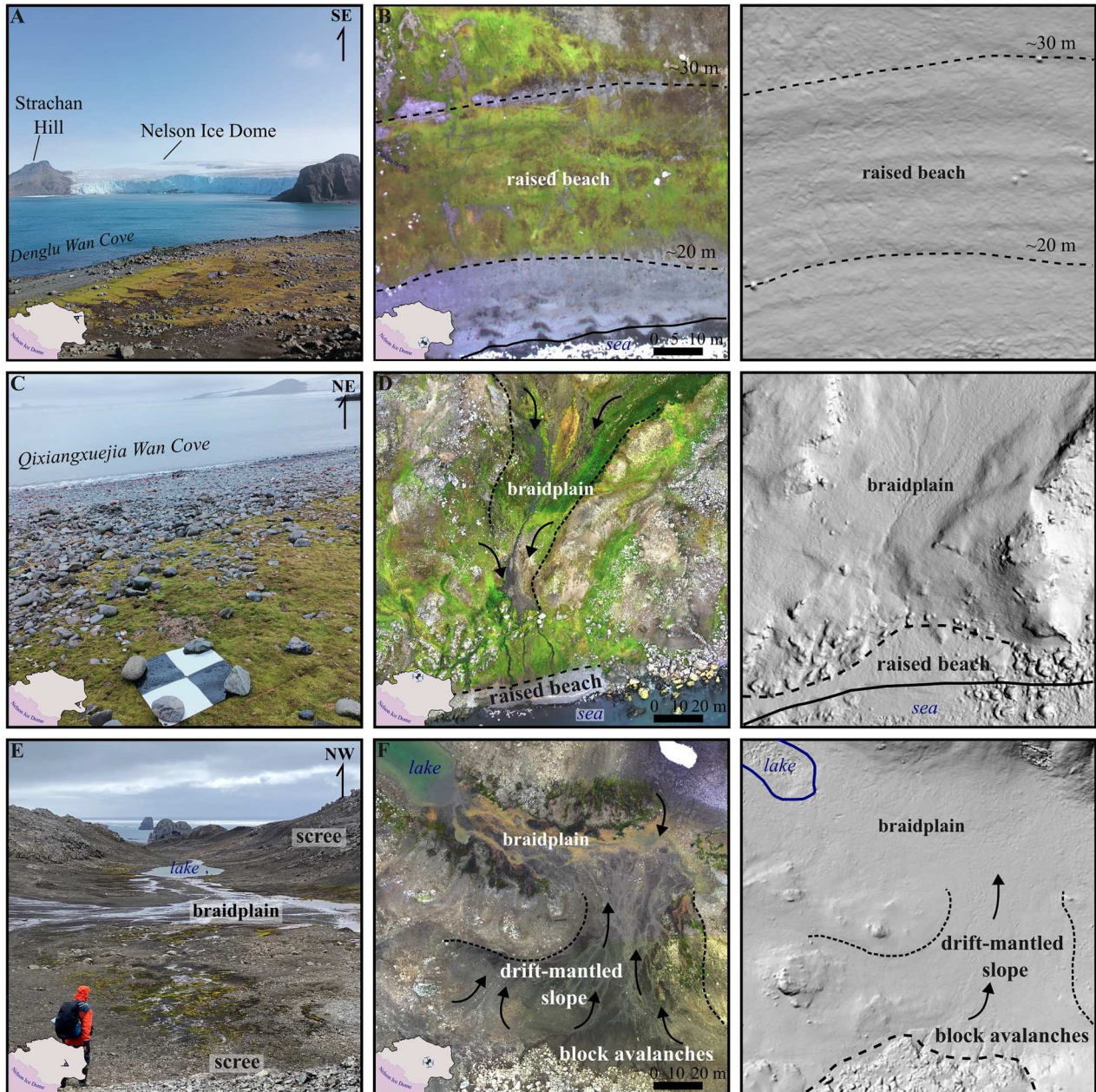


Figure 7. Representative paraglacial landforms and deposits in the study area, including coastal, marine, and glaciofluvial features. Hillshade maps in the right panel were derived from high-resolution drone-based DSMs (3 cm/px). A. South-eastward view of Denglu Wan Cove, displaying vegetated coastal zone with scattered debris blocks, and beach sediments; B. Orthomosaic and hillshade map of the same area as in A, highlighting the boundary between vegetated surfaces and beach deposits. Dashed lines indicate gradually elevated parts, interpreted as marine terraces. C. North-eastward view of Qixiangxuejia Wan Cove displays a well-sorted beach composed of pebbles and cobbles. D. Orthomosaic of the northern tip of Stansbury Peninsula, illustrating braided meltwater channels, moss-dominated vegetation, and waterlogged zones. E. North-westward view from Stansbury Peninsula, depicting a typical braidplain fed by meltwater into a small proglacial lake, with surrounding debris and rocky slopes. F. Orthomosaic of the same area as in D, displaying block avalanches and a drift-mantled slope carrying debris through the braidplain.

Raised beaches, which are former shorelines and now elevated above current sea level due to isostatic rebound, are widespread along the coast of the Stansbury Peninsula. These deposits consist predominantly of fine – to medium-grained sediments, but they are partly covered by blockfields, which are angular rock fragments resulting from frost weathering, particularly in gently sloped coastal areas (Figure 7A-C). At Quixiangxuejia Wan Cove, the coastline includes a well-developed beach ridge composed of well-sorted pebbles and cobbles, shaped by tidal activity and post-glacial sea-level changes (Figure 7C; Main Map).

Evidence of marine terraces, which are flat, step-like landforms representing former shore platforms,

is observed at sites such as Denglu Wan Cove, where a subtle increase in coastal elevation suggests uplifted former shorelines, although terrace stratigraphy is not always clearly visible (Figure 7B). Coastal areas generally show varying degrees of vegetation cover, with mosses and wetland vegetation (e.g. *Sanionia georgi-councinata* and *Warnstorfia* spp; Puhovkin et al., 2023), particularly evident in low-lying, waterlogged zones. One such example is the northern tip of Stansbury Peninsula, where braided meltwater channels flow towards the coast and are bordered by vegetation, including various colours of mosses and waterlogged areas (Figure 7D). Braidplains, the networks of shallow, gravel-bed meltwater channels, are also observed

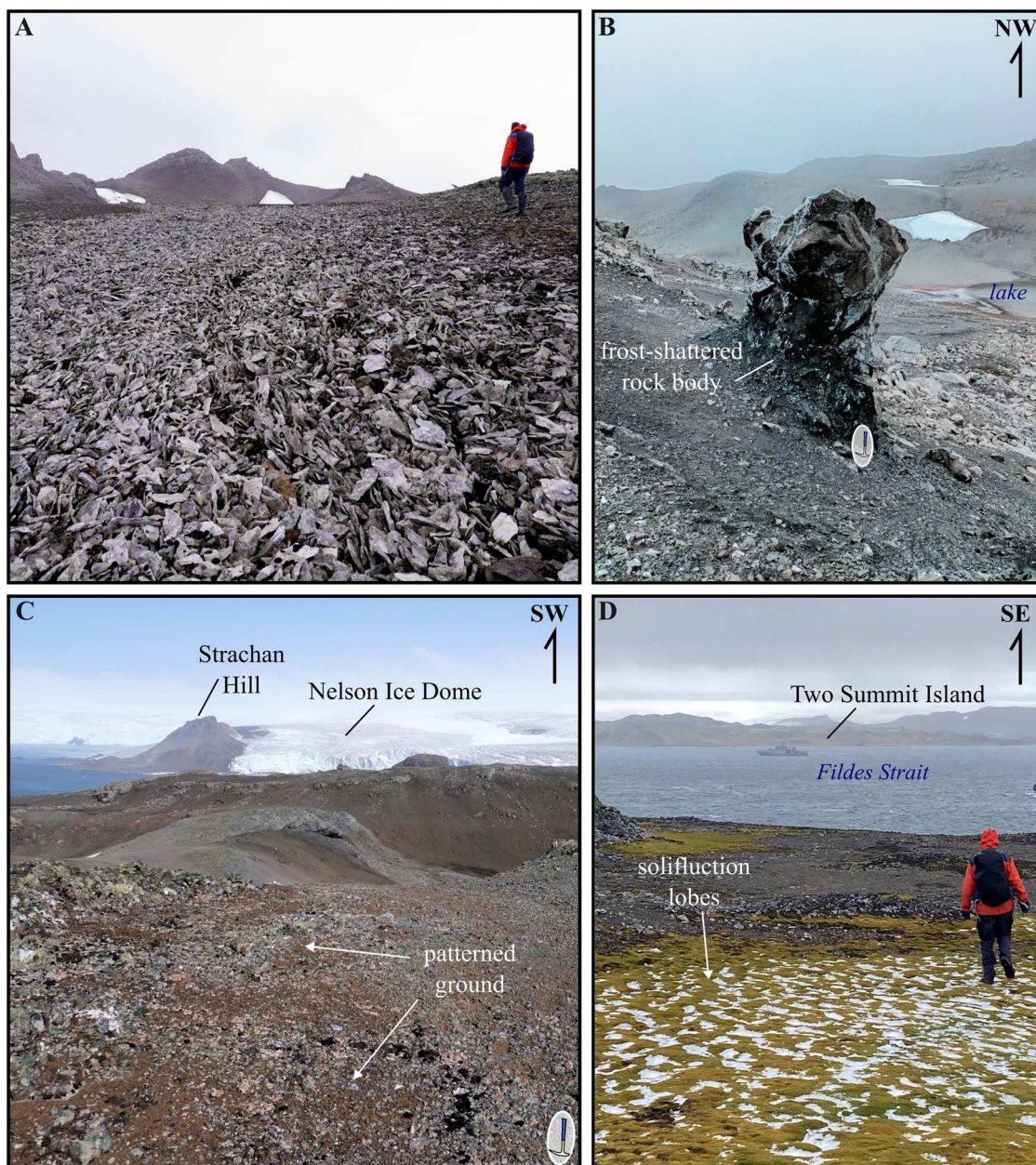


Figure 8. Typical periglacial landforms in the study area. A. Blockfield, consisting of angular, frost-shattered rocks, covers a gently sloped surface between mesas and raised beaches. B. An isolated frost-shattered rock body embedded within a scree slope. C. Patterned grounds observed on a mesa. D. Solifluction lobes on a slope between coast and mesas, with patchy snow and moss indicating active freeze-thaw processes. These features are better observed in drone-based orthomosaics (Figure 9).

within the bedrock valleys through the inner parts of Stansbury Peninsula (Figure 7E). Adjacent to these valleys, scree/talus slopes, which are the accumulations of angular rock debris, are also common (Figure 7E), while drift-mantled slopes, comprising glacial debris mixed with finer material, are apparent along the transitional margins between scree slopes and outwash plains (Figure 7F). In addition, block avalanches composed of fragmented rock blocks formed by large mass movements are observed in some of the scree slopes (Figure 7F).

4.2.4. Periglacial landforms and deposits

The periglacial landforms are widespread in the study area and include patterned grounds, solifluction lobes, rock stripes, blockfields (felsenmeer), and frost-shattered rock bodies (Figures 8 and 9; Main Map). Blockfields composed of angular rock fragments produced by frost weathering are especially common on

gently sloped areas between mesas and raised beaches (Figure 8A). These coarse, clast-dominated surfaces indicate long-term exposure to periglacial conditions and minimal sediment transport. The frost-shattered rock bodies, which are isolated, fractured outcrops often partially embedded within scree deposits, are also common (Figure 8B).

Patterned grounds are widespread, especially on the elevated mesas (80–120 m) and the low-lying central part (Main Map), and are characterised by clustered, circular rock patterns ranging in size from $\sim 1 \text{ m}^2$ to 10 m^2 , formed through repeated freeze–thaw processes (Figure 8C and Figure 9A–C). The solifluction lobes, appearing as curved, downslope ridges, are also found on gentle slopes (Figure 8D and Figure 9D–E). On steeper slopes, the rock stripes are evident, displaying sorted linear arrangements of coarse – and fine-grained materials, aligned parallel to the slope due to frost heave and gravity-driven processes (Figure 9F).

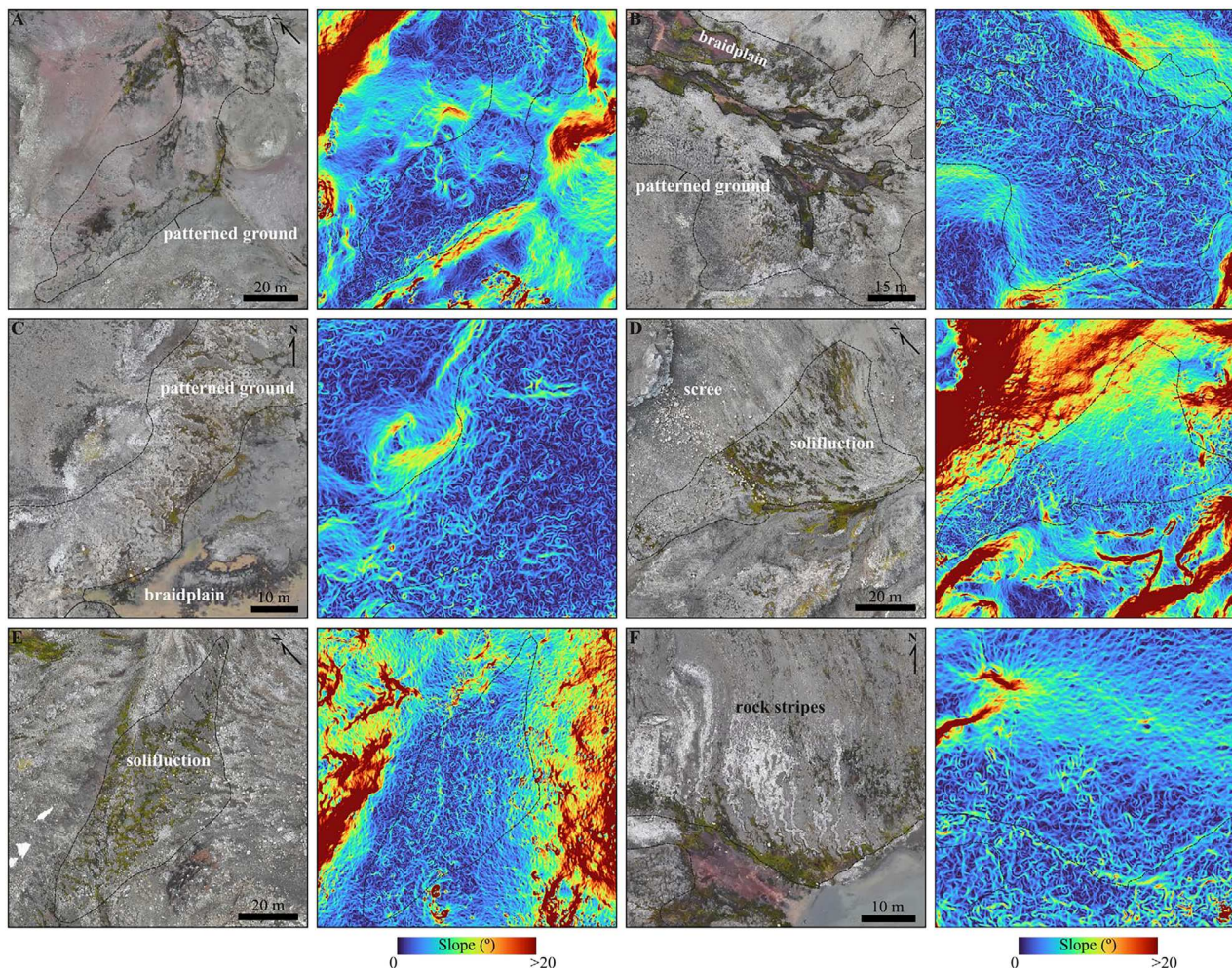


Figure 9. Orthomosaics and slope maps illustrate key periglacial landforms across the Stansbury Peninsula. A. Patterned ground on a gently slope surface, characterised by clustered, polygonal features; B. Patterned grounds interwoven with braidplains, highlighting the interaction between fluvial and periglacial processes; C. Patterned ground adjacent to a narrow braidplain channel, showing the relatively distinct boundary between sorted periglacial features and active fluvial zones; D. Well-developed solifluction lobes and a scree slope occupying a north-facing hillslope; E. Broad solifluction lobe complex on a gentle slope, with lobate structures extending downslope and clear evidence of vegetation patterning. F. Rock stripes developed along a moderate slope, featuring linear alternation of coarse rock fragments and finer-grained material aligned parallel to the slope aspect. The upper value in the slope maps attached to each orthomosaic is limited to 20° to better highlight the small-scale periglacial features.

5. Discussion and conclusions

This study presents the first detailed geomorphological maps of the proglacial landscapes in the northern part of Nelson Island (northern South Shetland Islands), namely Stansbury Peninsula and Cariz Cabo Cape (Main Map, Figures 2 and 3). The defined landforms reflect a complex interplay of glacial, proglacial, paraglacial, and periglacial processes, each leaving distinct imprints on the volcanic terrain. Overall, the landscape documents a history of multiple glacial advances and retreats during the Holocene, which are evident across the South Shetland Islands (Heredia Barión et al., 2023; Oliva et al., 2023; Palacios et al., 2020) and indeed the wider Antarctic Peninsula region (e.g. Carrivick et al., 2012; Guglielmin et al., 2016; Jennings et al., 2021). Furthermore, those changes observed on the South Shetland Islands, and documented in its geomorphology are likely to propagate south as temperatures rise (Stringer et al., 2025).

The moraines near current ice margins likely correspond to the most recent retreat phases following the Neoglaciation cold periods in the South Shetland Islands (~4.1 and 1 ka; Čejka et al., 2020; Palacios et al., 2020), while push moraines at lower slopes near outwash plains may also be tentatively correlated with these periods. The presence of polished and striated boulders on the coast and lower volcanic surfaces suggests they were previously subglacial, most likely during the Last Glacial Maximum, consistent with regional reconstructions indicating rapid retreat from a thicker ice sheet configuration (Cofaigh et al., 2014; Heroy & Anderson, 2007; Kaplan et al., 2020; Nývlt et al., 2020; Watcham et al., 2011).

The well-developed braided and outwash plains in the study area are similar to those observed on other nearby peninsulas, such as Fildes Peninsula, and throughout the South Shetland Islands (Heredia Barión et al., 2023; Li et al., 1996; Oliva & Ruiz-Fernández, 2017). These features indicate meltwater-driven deposition following the main phase of deglaciation (~9–6 ka; Heredia Barión et al., 2023; Oliva et al., 2019, 2023). These complex hydrological morphologies, shaped by both subglacial melt and surface run-off, reflect ongoing sediment fluxes modulated by ablation processes and seasonal melt pulses (e.g. Kavan et al., 2023).

Periglacial landforms (e.g. patterned ground, solifluction lobes, and blockfields) are prevalent in the Stansbury Peninsula and closely resemble those documented in other proglacial landscapes of the South Shetland Islands (Hall, 2002; López-Martínez et al., 2012). Patterned ground is most commonly found on elevated mesas, as in the case of other areas in the South Shetland Islands (Dąbski et al., 2017; López-Martínez et al., 2012), whereas solifluction lobes are typically located on scree slopes adjacent to proglacial environments. These landforms warrant further investigation into their dynamics,

which are closely related to topography, lithology, and environmental conditions (López-Martínez et al., 2012; Vieira et al., 2010). In addition, the identification of hyaloclastite and crystalline erratic boulders provides valuable evidence for reconstructing the deglacial history of the region.

Overall, our geomorphological map provides the first comprehensive overview of complex deglaciation processes and their imprints on the landforms of the Stansbury Peninsula. This map will certainly serve as a foundational dataset for future multidisciplinary studies in the region. As climate change continues to drive glacial retreat, such maps will be more critical for monitoring geomorphological changes and understanding the pace and effects of expanding proglacial landscapes across the Antarctic Peninsula.

Software

Maps were produced using QGIS 3.24.1-Tisler software, with further layout modifications via Inkscape 1.3.

Acknowledgment

The authors thank TÜBİTAK MAM Polar Research Institute (KARE), the Czech Antarctic Research Programme (CARP) and the Czech Antarctic Foundation for their support. Specifically, Vaclav Pavel, David Jindra, Ondrej Stanicky, Ondrej Zverina, Jan Havranek, and Anton Puhovkin for their great support during the field campaign in Nelson Island. David Jindra is thanked for producing high-resolution imagery of the study area. Pavel Kapler (CARP), Özgün Oktar and Doğaç Baybars İşler (KARE) are especially thanked for providing logistical and technical support. Many thanks to three reviewers (Werner Nel, Rosa Blanca Gonzalez, and Thomas Pingel) and the associate editor Jasper Knight for their constructive comments that significantly advance the manuscript.

Disclosure statement

No potential conflict of interest was reported by the author(s).

Funding

GU, BÖ (as the principal investigator), and partially AÜ were supported by the Turkish Polar Program, having been conducted since 2017 under the auspices of the Presidency of the Republic of Türkiye, under the responsibility of the Ministry of Industry and Technology, and coordinated by the TÜBİTAK MAM Polar Research Institute (KARE). CS was supported by Leeds-York-Hull Natural Environment Research Council (NERC) Doctoral Training Partnership (DTP) Panorama under Grant NE/S007458/1, The Ministry of Education, Youth and Sports of the Czech Republic project VAN 1/2023 and the Czech Antarctic Foundation.

Data availability statement

All data supporting the findings of this study are available within the article and its supplementary materials.

ORCID

Göksu Uslular  <http://orcid.org/0000-0001-8485-0093>
 Alp Ünal  <http://orcid.org/0000-0002-5078-9244>
 Christopher D. Stringer  <http://orcid.org/0000-0002-2902-9435>
 Daniel Nývlt  <http://orcid.org/0000-0002-6876-490X>
 Jonathan L. Carrivick  <http://orcid.org/0000-0002-9286-5348>
 Burcu Özsoy  <http://orcid.org/0000-0003-4320-1796>

References

- Amante, C., & Eakins, B. W. (2009). Etopo1 arc-minute global relief model: Procedures, data sources and analysis. *National Ocean and Atmospheric Administration*, p. 25.
- Ballantyne, C. K. (2002). Paraglacial geomorphology. *Quaternary Science Reviews*, 21(18–19), 1935–2017. [https://doi.org/10.1016/S0277-3791\(02\)00005-7](https://doi.org/10.1016/S0277-3791(02)00005-7)
- Bastías, J., Chew, D., Villanueva, C., Riley, T., Manfroi, J., Trevisan, C., Leppe, M., Castillo, P., Poblete, F., Tetzner, D., Giuliani, G., López, B., Chen, H., Zheng, G.-G., Zhao, Y., Gao, L., Rauch, A., & Jaña, R. (2023). The South Shetland Islands, Antarctica: Lithostratigraphy and geological map. *Frontiers in Earth Science*, 10, <https://doi.org/10.3389/feart.2022.1002760>
- Bemis, S. P., Mickelthwaite, S., Turner, D., James, M. R., Akciz, S., Thiele, S. T., & Bangash, H. A. (2014). Ground-based and UAV-based photogrammetry: A multi-scale, high-resolution mapping tool for structural geology and paleoseismology. *Journal of Structural Geology*, 69, 163–178. <https://doi.org/10.1016/j.jsg.2014.10.007>
- Burton-Johnson, A., Black, M., Fretwell, P. T., & Kaluza-Gilbert, J. (2016). An automated methodology for differentiating rock from snow, clouds and sea in Antarctica from landsat 8 imagery: A new rock outcrop map and area estimation for the entire antarctic continent. *The Cryosphere*, 10(4), 1665–1677. <https://doi.org/10.5194/tc-10-1665-2016>
- Carrivick, J. L., Davies, B. J., Glasser, N. F., Nývlt, D., & Hambrey, M. J. (2012). Late-Holocene changes in character and behaviour of land-terminating glaciers on James Ross Island, Antarctica. *Journal of Glaciology*, 58(212), 1176–1190. <https://doi.org/10.3189/2012JoG11J148>
- Carrivick, J. L., Heckmann, T., Turner, A., & Fischer, M. (2018). An assessment of landform composition and functioning with the first proglacial systems dataset of the central European Alps. *Geomorphology*, 321, 117–128. <https://doi.org/10.1016/j.geomorph.2018.08.030>
- Carrivick, J. L., Smith, M. W., & Quincey, D. J. (2016). *Structure from motion in the geosciences*. John Wiley & Sons.
- Carrivick, J. L., Smith, M. W., Quincey, D. J., & Carver, S. J. (2013). Developments in budget remote sensing for the geosciences. *Geology Today*, 29(4), 138–143. <https://doi.org/10.1111/gto.12015>
- Carrivick, J. L., & Tweed, F. S. (2013). Proglacial lakes: Character, behaviour and geological importance. *Quaternary Science Reviews*, 78, 34–52. <https://doi.org/10.1016/j.quascirev.2013.07.028>
- Carrivick, J. L., & Tweed, F. S. (2021). Deglaciation controls on sediment yield: Towards capturing spatio-temporal variability. *Earth-Science Reviews*, 221, 103809. <https://doi.org/10.1016/j.earscirev.2021.103809>
- Čejka, T., Nývlt, D., Kopalová, K., Bulínová, M., Kavan, J., Lirio, J. M., Coria, S. H., & van de Vijver, B. (2020). Timing of the neoglacial onset on the North-Eastern Antarctic Peninsula based on lacustrine archive from Lake Anónima, Vega Island. *Global and Planetary Change*, 184, 103050. <https://doi.org/10.1016/j.gloplacha.2019.103050>
- Chandler, B. M. P., Lovell, H., Boston, C. M., Lukas, S., Barr, I. D., Benediktsson, ÍÖ, Benn, D. I., Clark, C. D., Darvill, C. M., Evans, D. J. A., Ewertowski, M. W., Loibl, D., Margold, M., Otto, J.-C., Roberts, D. H., Stokes, C. R., Storrar, R. D., & Stroeven, A. P. (2018). Glacial geomorphological mapping: A review of approaches and frameworks for best practice. *Earth-Science Reviews*, 185, 806–846. <https://doi.org/10.1016/j.earscirev.2018.07.015>
- Cofaigh, CÖ, Davies, B. J., Livingstone, S. J., Smith, J. A., Johnson, J. S., Hocking, E. P., Hodgson, D. A., Anderson, J. B., Bentley, M. J., Canals, M., Domack, E., Dowdeswell, J. A., Evans, J., Glasser, N. F., Hillenbrand, C.-D., Larter, R. D., Roberts, S. J., & Simms, A. R. (2014). Reconstruction of ice-sheet changes in the Antarctic Peninsula since the Last Glacial Maximum. *Quaternary Science Reviews*, 100, 87–110. <https://doi.org/10.1016/j.quascirev.2014.06.023>
- Convey, P. (2010). Terrestrial biodiversity in Antarctica – recent advances and future challenges. *Polar Science*, 4(2), 135–147. <https://doi.org/10.1016/j.polar.2010.03.003>
- Corte, E., Ajmar, A., Camporeale, C., Cina, A., Coviello, V., Giulio Tonolo, F., Godio, A., Macelloni, M. M., Tamea, S., & Vergnano, A. (2024). Multitemporal characterization of a proglacial system: A multidisciplinary approach. *Earth System Science Data*, 16(7), 3283–3306. <https://doi.org/10.5194/essd-16-3283-2024>
- Dąbski, M., Zmarz, A., Pabjanek, P., Korczak-Abshire, M., Karsznia, I., & Chwedorzewska, K. J. (2017). UAV-based detection and spatial analyses of periglacial landforms on Demay Point (King George Island, South Shetland Islands, Antarctica). *Geomorphology*, 290, 29–38. <https://doi.org/10.1016/j.geomorph.2017.03.033>
- da Rosa, C. N., Pereira Filho, W., Bremer, U. F., Putzke, J., de Andrade, A. M., Kramer, G., Hillebrand, F. L., & de Jesus, J. B. (2022). Spectral behavior of vegetation in Harmony Point, Nelson Island, Antarctica. *Biodiversity and Conservation*, 31(7), 1867–1885. <https://doi.org/10.1007/s10531-022-02408-7>
- Ely, J. C., Graham, C., Barr, I. D., Rea, B. R., Spagnolo, M., & Evans, J. (2017). Using UAV acquired photography and structure from motion techniques for studying glacier landforms: Application to the glacial flutes at Isfallsgläciären. *Earth Surface Processes and Landforms*, 42(6), 877–888. <https://doi.org/10.1002/esp.4044>
- Francelino, M. R., Schaefer, C. E. G. R., Simas, F. N. B., Filho, E. I. F., De Souza, J. J. L., & Da Costa, L. M. (2011). Geomorphology and soils distribution under paraglacial conditions in an ice-free area of Admiralty Bay, King George Island, Antarctica. *CATENA*, 85(3), 194–204. <https://doi.org/10.1016/j.catena.2010.12.007>
- Gao, L., Zhao, Y., Yang, Z., Liu, J., Liu, X., Zhang, S., & Pei, J. (2018). New Paleomagnetic and 40Ar/39Ar Geochronological results for the South Shetland Islands, West Antarctica, and their tectonic implications. *Journal of Geophysical Research: Solid Earth*, 123(1), 4–30. <https://doi.org/10.1002/2017JB014677>
- Guglielmin, M., Convey, P., Malfasi, F., & Cannone, N. (2016). Glacial fluctuations since the ‘Medieval Warm Period’ at Rothera Point (western Antarctic Peninsula). *The Holocene*, 26(1), 154–158. <https://doi.org/10.1177/0959683615596827>
- Hall, K. (2002). Review of present and quaternary periglacial processes and landforms of the maritime and sub-Antarctic region: Periglacial and Permafrost

- Research in the Southern Hemisphere. *South African Journal of Science*, 98(1), 71–81. <https://doi.org/10.10520/EJC97386>
- Heckmann, T., McColl, S., & Morche, D. (2016). Retreating ice: Research in pro-glacial areas matters. *Earth Surface Processes and Landforms*, 41(2), 271–276. <https://doi.org/10.1002/esp.3858>
- Heredia Barión, P., Roberts, S. J., Spiegel, C., Binnie, S. A., Wacker, L., Davies, J., Gabriel, I., Jones, V. J., Blockley, S., Pearson, E. J., Foster, L., Davies, S. J., Roland, T. P., Hocking, E. P., Bentley, M. J., Hodgson, D. A., Hayward, C. L., McCulloch, R. D., Strelin, J. A., & Kuhn, G. (2023). Holocene deglaciation and glacier readvances on the Fildes Peninsula and King George Island (Isla 25 de Mayo), South Shetland Islands, NW Antarctic Peninsula. *The Holocene*, 33(6), 636–658. <https://doi.org/10.1177/09596836231157059>
- Heroy, D. C., & Anderson, J. B. (2007). Radiocarbon constraints on Antarctic Peninsula Ice Sheet retreat following the Last Glacial Maximum (LGM). *Quaternary Science Reviews*, 26(25), 3286–3297. <https://doi.org/10.1016/j.quascirev.2007.07.012>
- Howat, I. M., Porter, C., Smith, B. E., Noh, M.-J., & Morin, P. (2019). The reference elevation model of Antarctica. *The Cryosphere*, 13(2), 665–674. <https://doi.org/10.5194/tc-13-665-2019>
- Jennings, S. J. A., Davies, B. J., Nývlt, D., Glasser, N. F., Engel, Z., Hrbáček, F., Carrivick, J. L., Mlčoch, B., & Hambrey, M. J. (2021). Geomorphology of Ulu Peninsula, James Ross Island, Antarctica. *Journal of Maps*, 17(2), 125–139. <https://doi.org/10.1080/17445647.2021.1893232>
- Jiawen, R., Dahe, Q., Petit, J. R., Jouzel, J., Wenti, W., Chen, L., Xiaojun, W., Songlin, Q., & Xiaoxiang, W. (1995). Glaciological studies on Nelson Island, South Shetland Islands, Antarctica. *Journal of Glaciology*, 41(138), 408–412. <https://doi.org/10.3189/S0022143000016270>
- Kaplan, M. R., Strelin, J. A., Schaefer, J. M., Peltier, C., Martini, M. A., Flores, E., Winckler, G., & Schwartz, R. (2020). Holocene glacier behavior around the northern Antarctic Peninsula and possible causes. *Earth and Planetary Science Letters*, 534, 116077. <https://doi.org/10.1016/j.epsl.2020.116077>
- Kavan, J., Hrbáček, F., & Stringer, C. D. (2023). Proglacial streams runoff dynamics in Devil's Bay, Vega Island, Antarctica. *Hydrological Sciences Journal*, 68(7), 967–981. <https://doi.org/10.1080/02626667.2023.2195559>
- Kavan, J., Ondruch, J., Nývlt, D., Hrbáček, F., Carrivick, J. L., & Láška, K. (2017). Seasonal hydrological and suspended sediment transport dynamics in proglacial streams, James Ross Island, Antarctica. *Geografiska Annaler: Series A, Physical Geography*, 99(1), 38–55. <https://doi.org/10.1080/04353676.2016.1257914>
- Li, Z. N., Zheng, X. S., Liu, X. H., Jin, Q. M., Li, G., & Shang, R. X. (1996). Geological map of the Fildes peninsula, King George Island and Stansbury Peninsula. *Nelson Island, Antarctica: Geological House*.
- López-Martínez, J., Schmid, T., Serrano, E., Mink, S., Nieto, A., & Guillaso, S. (2016). Geomorphology and landforms distribution in selected ice-free areas in the South Shetland Islands, Antarctic Northern Peninsula region. *Cuadernos de Investigación Geográfica*, 42(2), 435–455. <https://doi.org/10.18172/cig.2965>
- López-Martínez, J., Serrano, E., Schmid, T., Mink, S., & Linés, C. (2012). Periglacial processes and landforms in the South Shetland Islands (Northern Antarctic Peninsula Region). *Geomorphology*, 155–156, 62–79. <https://doi.org/10.1016/j.geomorph.2011.12.018>
- Mansilla, H. G., Stinnesbeck, W., Varela, N., & Leppe, M. (2014). Eocene fossil feather from King George Island, South Shetland Islands, Antarctica. *Antarctic Science*, 26(4), 384–388. <https://doi.org/10.1017/S0954102013000771>
- Matsuoka, K., Skoglund, A., Roth, G., de Pomereu, J., Griffiths, H., Headland, R., Herried, B., Katsumata, K., Le Brocq, A., Licht, K., & Morgan, F. (2021). Quantarctica, an integrated mapping environment for Antarctica, the Southern Ocean, and sub-Antarctic Islands. *Environmental Modelling & Software*, 140, 105015. <https://doi.org/10.1016/j.envsoft.2021.105015>
- Meier, M., Francelino, M. R., Gasparini, A. S., Thomazini, A., Pereira, A. B., Von Krüger, F. L., Fernandes-Filho, E. I., & Schaefer, C. E. G. R. (2023). Soils and geoenvironments at Stansbury Peninsula, Nelson Island, maritime Antarctica. *CATENA*, 223, 106884. <https://doi.org/10.1016/j.catena.2022.106884>
- Neznajová, Z. (2024). *Analýza teplotních a vlhkostních poměrů na dvou rozdílných lokalitách v oblasti Antarktického poloostrova (In Czech)* [BSc. Thesis]. Masaryk University.
- Nývlt, D., Glasser, N. F., Hocking, E., Oliva, M., Roberts, S. J., & Roman, M. (2020). Chapter 5 – tracing the deglaciation since the last glacial maximum. In M. Oliva, & J. Ruiz-Fernández (Eds.), *Past Antarctica* (pp. 89–107). Academic Press.
- Oliva, M., Antoniadou, D., Serrano, E., Giral, S., Liu, E. J., Granados, I., Pla-Rabes, S., Toro, M., Hong, S. G., & Vieira, G. (2019). The deglaciation of Barton Peninsula (King George Island, South Shetland Islands, Antarctica) based on geomorphological evidence and lacustrine records. *Polar Record*, 55(3), 177–188. <https://doi.org/10.1017/S0032247419000469>
- Oliva, M., Palacios, D., Fernández-Fernández, J. M., Fernandes, M., Schimmelpfennig, I., Vieira, G., Antoniadou, D., Pérez-Alberti, A., García-Oteyza, J., & ASTER TEAM (2023). Holocene deglaciation of the northern Fildes Peninsula, King George Island, Antarctica. *Land Degradation & Development*, 34(13), 3973–3990. <https://doi.org/10.1002/ldr.4730>
- Oliva, M., & Ruiz-Fernández, J. (2017). Geomorphological processes and frozen ground conditions in Elephant Point (Livingston Island, South Shetland Islands, Antarctica). *Geomorphology*, 293, 368–379. <https://doi.org/10.1016/j.geomorph.2016.01.020>
- Oosthuizen, W. C., Krüger, L., Jouanneau, W., & Lowther, A. D. (2020). Unmanned aerial vehicle (UAV) survey of the Antarctic shag (*Leucocarbo bransfieldensis*) breeding colony at Harmony Point, Nelson Island, South Shetland Islands. *Polar Biology*, 43(2), 187–191. <https://doi.org/10.1007/s00300-019-02616-y>
- Orwin, J. F., & Smart, C. C. (2004). Short-term spatial and temporal patterns of suspended sediment transfer in proglacial channels, small River Glacier, Canada. *Hydrological Processes*, 18(9), 1521–1542. <https://doi.org/10.1002/hyp.1402>
- Palacios, D., Ruiz-Fernández, J., Oliva, M., Andrés, N., Fernández-Fernández, J. M., Schimmelpfennig, I., Leanni, L., & González-Díaz, B. (2020). Timing of formation of neoglacial landforms in the South Shetland Islands (Antarctic Peninsula): Regional and global implications. *Quaternary Science Reviews*, 234, 106248. <https://doi.org/10.1016/j.quascirev.2020.106248>
- Puhovkin, A., Smykla, J., Váczi, P., & Parnikoza, I. (2023). Spectral characteristics of bryophyte carpet and mat subformation showing a vitality-dependent color pattern:

- Comparison for two distant regions of maritime Antarctica. *Czech Polar Reports*, 13(1), Article 1. <https://doi.org/10.5817/CPR2023-1-9>
- Renssen, H., Seppä, H., Crosta, X., Goosse, H., & Roche, D. M. (2012). Global characterization of the Holocene Thermal Maximum. *Quaternary Science Reviews*, 48, 7–19. <https://doi.org/10.1016/j.quascirev.2012.05.022>
- Rodrigues, W. F., Oliveira, F. S., Schaefer, C. E. G. R., Leite, M. G. P., Gauzzi, T., Bockheim, J. G., & Putzke, J. (2019). Soil-landscape interplays at Harmony Point, Nelson Island, Maritime Antarctica: Chemistry, mineralogy and classification. *Geomorphology*, 336, 77–94. <https://doi.org/10.1016/j.geomorph.2019.03.030>
- Roland, T. P., Bartlett, O. T., Charman, D. J., Anderson, K., Hodgson, D. A., Amesbury, M. J., Maclean, I., Fretwell, P. T., & Fleming, A. (2024). Sustained greening of the Antarctic Peninsula observed from satellites. *Nature Geoscience*, 17(11), 1121–1126. <https://doi.org/10.1038/s41561-024-01564-5>
- SCAR. (2014). *Composite Gazetteer of Antarctica [GCMD Metadata]*. Scientific Committee on Antarctic Research.
- Slaymaker, O. (2009). Proglacial, periglacial or paraglacial? *Geological Society, London, Special Publications*, 320(1), 71–84. <https://doi.org/10.1144/SP320.6>
- Slaymaker, O. (2011). Criteria to distinguish between periglacial, proglacial and paraglacial environments. *QUAGEO*, 30(1), 85–94. <https://doi.org/10.2478/v10117-011-0008-y>
- Smith, M. W., Carrivick, J. L., & Quincey, D. J. (2016). Structure from motion photogrammetry in physical geography. *Progress in Physical Geography: Earth and Environment*, 40(2), 247–275. <https://doi.org/10.1177/0309133315615805>
- Smith, M. J., & Clark, C. D. (2005). Methods for the visualization of digital elevation models for landform mapping. *Earth Surface Processes and Landforms*, 30(7), 885–900. <https://doi.org/10.1002/esp.1210>
- Stringer, C. D., Boyle, J. F., Hrbáček, F., Láška, K., Neděľčev, O., Kavan, J., Kňažková, M., Carrivick, J. L., Quincey, D. J., & Nývlt, D. (2024). Quantifying sediment sources, pathways, and controls on fluvial transport dynamics on James Ross Island, Antarctica. *Journal of Hydrology*, 635, 131157. <https://doi.org/10.1016/j.jhydrol.2024.131157>
- Stringer, C. D., Carrivick, J. L., Quincey, D. J., Nývlt, D., & Comber, A. (2025). Land cover change across the major proglacial regions of the sub-Antarctic islands, Antarctic Peninsula, and McMurdo Dry Valleys, during the 21st century. *Arctic, Antarctic, and Alpine Research*, 57(1), 2483474. <https://doi.org/10.1080/15230430.2025.2483474>
- Vaughan, D. G., Marshall, G. J., Connolley, W. M., Parkinson, C., Mulvaney, R., Hodgson, D. A., King, J. C., Pudsey, C. J., & Turner, J. (2003). Recent rapid regional climate warming on the Antarctic Peninsula. *Climatic Change*, 60(3), 243–274. <https://doi.org/10.1023/A:1026021217991>
- Vieira, G., Bockheim, J., Guglielmin, M., Balks, M., Abramov, A. A., Boelhouwers, J., Cannone, N., Ganzert, L., Gilichinsky, D. A., Goryachkin, S., López-Martínez, J., Meiklejohn, I., Raffi, R., Ramos, M., Schaefer, C., Serrano, E., Simas, F., Sletten, R., & Wagner, D. (2010). Thermal state of permafrost and active-layer monitoring in the antarctic: Advances during the international polar year 2007–2009. *Permafrost and Periglacial Processes*, 21(2), 182–197. <https://doi.org/10.1002/ppp.685>
- Watcham, E. P., Bentley, M. J., Hodgson, D. A., Roberts, S. J., Fretwell, P. T., Lloyd, J. M., Larter, R. D., Whitehouse, P. L., Leng, M. J., Monien, P., & Moreton, S. G. (2011). A new Holocene relative sea level curve for the South Shetland Islands, Antarctica. *Quaternary Science Reviews*, 30(21–22), 3152–3170. <https://doi.org/10.1016/j.quascirev.2011.07.021>
- Xiangshen, Z., & Xiaohan, L. (1990). Geology of fildes Peninsula, King George Island, West Antarctica – A study on the stratigraphy and volcanism. *Antarctic Research*, 1(1), 8–19.
- Xiaodong, L., Liguang, S., & Xuebin, Y. (2004). Textural and geochemical characteristics of proglacial sediments: A case study in the foreland of the Nelson Ice Cap, Antarctica. *Acta Geologica Sinica – English Edition*, 78(4), 970–981. <https://doi.org/10.1111/j.1755-6724.2004.tb00219.x>
- Yıldırım, C. (2020). Geomorphology of Horseshoe Island, Marguerite Bay, Antarctica. *Journal of Maps*, 16(2), 56–67. <https://doi.org/10.1080/17445647.2019.1692700>
- Zimmer, A., Beach, T., Klein, J. A., & Recharte Bullard, J. (2022). The need for stewardship of lands exposed by deglaciation from climate change. *WIREs Climate Change*, 13(2), e753. <https://doi.org/10.1002/wcc.753>